Probing photonic content of the proton using photon-induced dilepton production in $p+\mathrm{Pb}$ collisions at the LHC

M. Dyndal and A. Glazov

DESY

M. Luszczak and R. Sadykov

.

Abstract

We propose a new experimental method to validate photon parton distribution function (PDF) inside the proton at LHC energies. It is based on the measurement of dilepton production from the $\gamma p \to \ell^+\ell^- + X$ reaction in proton–lead collisions. These experimental conditions guarantee relatively clean environment, both in terms of reconstruction of the final state and in terms of possible background. We firstly calculate the cross sections for this process with collinear photon PDFs, where we identify correct choice of the scale, in analogy to deep inelastic scattering kinematics. We then include the virtuality of probed photon in the calculations, based on modern parameterizations of deep inelastic structure functions. Finally, we find that significant rates of this process are accessible by LHC experiments with existing datasets.

I. INTRODUCTION

Precise calculations of various electroweak reactions in pp collisions at the LHC need to account for, on top of the higher-order corrections, the effects of photon-induced subprocesses. The relevant examples are the production of lepton pairs [1–5] or pairs of electroweak bosons [6–13].

Recently, a precise photon distribution inside the proton has been evaluated in Ref. [14]. This approach provides a model-independent determination of the photon PDF (embedded in so-called LUXqed distribution) and it is based on proton structure function and elastic form factor fits in electron–proton scattering.

Up to date, there are no experimentally clean processes identified that would allow to either strongly constrain or verify the calculations. For example, the extraction of photon PDF from isolated photon production in deep inelastic scattering (DIS) [15] or from inclusive $pp \to \ell^+\ell^- + X$ reaction [2, 16, 17] is limited due to large QCD background. On contrary, the elastic part of the photon PDF is verified via exclusive $\gamma\gamma \to \ell^+\ell^-$ process, measured in pp collisions by ATLAS [18, 19], CMS [20, 21] and recently by CMS+TOTEM [22] collaborations.

We therefore propose a new experimental method to constrain photonic content of the proton. Thanks to the large fluxes of quasi-real photons from the Pb ion at the LHC, the photon-induced dilepton production in p + Pb collision configuration is a very clean way to probe photon PDF. This process is shown schematically in Fig. 1, where by analogy to DIS, two leading-order diagrams can be identified. Since the photon flux from the ion scales with Z^2 and QCD-induced cross-sections scale approximately with A, the amount of QCD background is greatly reduced comparing to pp case.

Moreover, as this process does not involve the exchange of color with the photon-emitting nucleus, no significant particle production is expected in the rapidity region between the dilepton system and the nucleus. The photon-emitting nucleus is also expected to produce no neutrons because the photons couple to the entire nucleus. Thus, a combination of a rapidity gap and zero neutrons in the same direction provide straightforward criteria to identify these events experimentally.

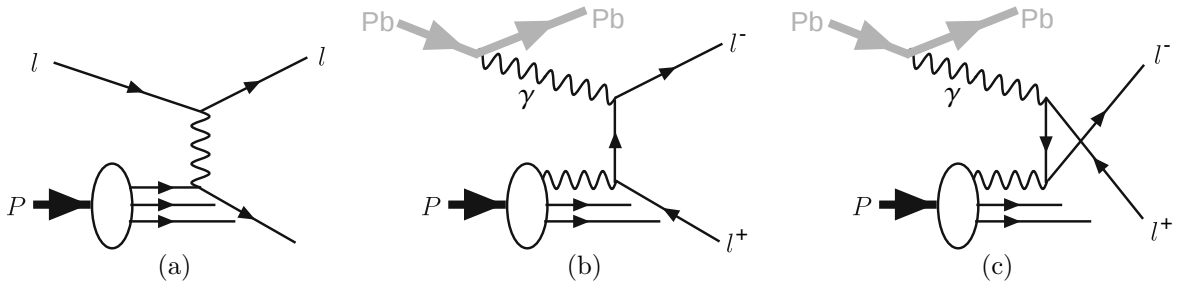

FIG. 1: Schematic graphs for deep inelastic scattering, $\ell^{\pm}p \to \ell^{\pm} + X$ (a) and photon-induced dilepton prodcution, $\gamma p \to \ell^+\ell^- + X$, in $p+\mathrm{Pb}$ collisions for t-channel (b) and u-channel (c) lepton exchange.

II. FORMALISM

A. Elastic vertices

In this work we are only interested in the elastic vertices on the nucleus side.

We recall, that for the proton, we can express the photon flux through the electric and magnetic form factors $G_E(Q^2)$ and $G_M(Q^2)$ of the proton:

$$W_T^{\mathrm{el}}(M_X^2, Q^2) = \delta(M_X^2 - m_p^2)\, Q^2 G_M^2(Q^2)\,,\; W_L^{\mathrm{el}}(M_X^2, Q^2) = \delta(M_X^2 - m_p^2) 4m_p^2 G_E^2(Q^2)\,. \quad (1)$$

The contribution to the photon flux is then again obtained by contracting

$$\frac{p^\mu p^\nu}{s^2}\, W_{\mu\nu}^{\mathrm{el}}(M_X^2, Q^2) = \delta(M_X^2 - m_p^2)\Big[\Big(1 - \frac{z}{2}\Big)^2 \frac{4m_p^2 G_E^2(Q^2) + Q^2 G_M^2(Q^2)}{4m_p^2 + Q^2} + \frac{z^2}{4} G_M^2(Q^2)\Big] \quad (2)$$

For the nucleus, we follow [23], and replace

$$\frac{4m_p^2 G_E^2(Q^2) + Q^2 G_M^2(Q^2)}{4m_p^2 + Q^2} \longrightarrow Z^2 F_{\mathrm{em}}^2(Q^2)\,. \quad (3)$$

We neglect the magnetic form factor in the following. (It even rigorously vanishes for spinless nuclei.)

For the ^{208}Pb nucleus, we use the realistic formfactor from the STARLIGHT MC.

$$F_{\mathrm{em}}(Q^2) = \frac{3}{(QR_A)^3}\Big\{\sin(QR_A) - QR_A\cos(QR_A)\Big\}\frac{1}{1 + a^2Q^2}\,. \quad (4)$$

Here

$$R_A = 1.1A^{1/3}\,\mathrm{fm}\,,\; a = 0.7\,\mathrm{fm},\; Q = \sqrt{Q^2}\,. \quad (5)$$

Therefore we obtain the elastic flux

$$\mathcal{F}^{\rm el}_{\gamma^*\leftarrow A}(z,\boldsymbol{q}) = \frac{Z^2\alpha_{\rm em}}{\pi}\,(1-z)\,\Big(\frac{\boldsymbol{q}^2}{\boldsymbol{q}^2+z(M_X^2-m_A^2)+z^2m_A^2}\Big)^2\,F^2_{\rm em}(Q^2)\,. \tag{6}$$

For ^{208}Pb the charge is $Z=82$.

B. Inelastic vertices

We consider the inelastic processes with breakup of a proton. Then the hadronic tensor is expressed in terms of the electromagnetic currents as:

$$W^{\rm in}_{\mu\nu}(M_X^2,Q^2) = \overline{\sum_X}(2\pi)^3\,\delta^{(4)}(p_X-p_A-q)\,\langle p|J_\mu|X\rangle\langle X|J^\dagger_\nu|p\rangle\,d\Phi_X\,, \tag{7}$$

and its elements can be measured in inclusive electron scattering off the target. We wish to express it in terms of the virtual photoabsorption cross section of transverse and longitudinal photons. To this end we introduce the covariant vectors tensors

$$e^{(0)}_\mu = \sqrt{\frac{Q^2}{X}}\Big(p_{A\mu}-\frac{(p_A\cdot q)}{q^2}q_\mu\Big)\,,\; X=(p_A\cdot q)^2+m_A^2Q^2\,,\; e^{(0)}\cdot e^{(0)}=+1\,, \tag{8}$$

and

$$\delta^\perp_{\mu\nu}(p_A,q) = g_{\mu\nu}-\frac{q_\mu q_\nu}{q^2}-e^{(0)}_\mu e^{(0)}_\nu\,. \tag{9}$$

Here $\delta^\perp_{\mu\nu}$ projects on photons carrying helicity ±1 in the γ^*p-cms frame, and $e^{(0)}_\mu$ plays the role of the polarization vector of the longitudinal photon. Notice that $q\cdot e^0 = q^\mu\delta^\perp_{\mu\nu}=0$, so that the hadronic tensor has the convenient gauge invariant decomposition

$$W^{\rm in}_{\mu\nu}(M_X^2,Q^2) = -\delta^\perp_{\mu\nu}(p_A,q)\,W^{\rm in}_T(M_X^2,Q^2)+e^{(0)}_\mu e^{(0)}_\nu\,W^{\rm in}_L(M_X^2,Q^2)\,. \tag{10}$$

The virtual photoabsorption cross sections are defined as

$$\begin{aligned}\sigma_T(\gamma^*p) &= \frac{4\pi\alpha_{\rm em}}{4\sqrt{X}}\Big(-\frac{\delta^\perp_{\mu\nu}}{2}\Big)2\pi W^{\rm in}_{\mu\nu}(M_X^2,Q^2)\\ \sigma_L(\gamma^*p) &= \frac{4\pi\alpha_{\rm em}}{4\sqrt{X}}\,e^0_\mu e^0_\nu\,2\pi W^{\rm in}_{\mu\nu}(M_X^2,Q^2)\,.\end{aligned} \tag{11}$$

It is customary to introduce dimensionless structure function $F_i(x_{\rm Bj},Q^2), i=T,L$ as

$$\sigma_{T,L}(\gamma^*p) = \frac{4\pi^2\alpha_{\rm em}}{Q^2}\,\frac{1}{\sqrt{1+\frac{4x^2_{\rm Bj}m_A^2}{Q^2}}}\,F_{T,L}(x_{\rm Bj},Q^2)\,, \tag{12}$$

where

$$x_{\rm Bj} = \frac{Q^2}{Q^2 + M_X^2 - m_A^2}\,. \tag{13}$$

Then, our structure functions $W_{T,L}$ are expressed through the more conventional $F_{T,L}$ as

$$W^{\rm in}_{T,L}(M_X^2, Q^2) = \frac{1}{x_{\rm Bj}}\, F_{T,L}(x_{\rm Bj}, Q^2)\,. \tag{14}$$

In the literature one often finds rather $F_1(x_{\rm Bj}, Q^2), F_2(x_{\rm Bj}, Q^2)$ structure functions, which are related to $F_{T,L}$ through

$$\begin{aligned} F_T(x_{\rm Bj}, Q^2) &= 2x_{\rm Bj} F_1(x_{\rm Bj}, Q^2)\,, \\ F_2(x_{\rm Bj}, Q^2) &= \frac{F_T(x_{\rm Bj}, Q^2) + F_L(x_{\rm Bj}, Q^2)}{1 + \frac{4x_{\rm Bj}^2 m_A^2}{Q^2}}\,. \end{aligned} \tag{15}$$

Now, performing the contraction with $p_B^\mu p_B^\nu$, we get

$$\frac{p_B^\mu p_B^\nu}{s^2}\, W^{\rm in}_{\mu\nu}(M_X^2, Q^2) = \Big(1 - \frac{z}{x_{\rm Bj}} + \frac{z^2}{4x_{\rm Bj}^2}\Big)\frac{F_2(x_{\rm Bj}, Q^2)}{Q^2 + M_X^2 - m_p^2} + \frac{z^2}{4x_{\rm Bj}^2}\frac{2x_{\rm Bj}F_1(x_{\rm Bj}, Q^2)}{Q^2 + M_X^2 - m_p^2}\,. \tag{16}$$

In the deep inelastic region $F_2 \sim F_T + F_L$, and using $2x_{\rm Bj}F_1 \sim F_2$ in the second term, we can write more succinctly

$$\frac{p_B^\mu p_B^\nu}{s^2}\, W^{\rm in}_{\mu\nu}(M_X^2, Q^2) = Q^2 \cdot f_T\Big(\frac{z}{x_{\rm Bj}}\Big)\, x_{\rm Bj} F_2(x_{\rm Bj}, Q^2)\,, \tag{17}$$

with

$$f_T(y) = 1 - y + y^2/2 = \frac{1}{2}\Big[1 + (1-y)^2\Big]\,. \tag{18}$$

C. Collinear-factorization approach

Production of lepton pairs at large transverse momenta is a hard process, to which standard arguments for factorization apply, and collinear factorization should be an appropriate starting point to calculate e.g. rapidity or transverse momentum spectra of leptons. In fact, the dominant contribution to large-invariant mass dilepton pairs is of course the well known Drell-Yan process, but nothing prevents us from also including photon as partons along with quarks and gluons.

Then the photon parton distribution, $\gamma(z,Q^2)$, of photons carrying a fraction z of the proton's light-cone momentum, obeys the DGLAP equation,

$$\begin{aligned}\frac{d\gamma(z,Q^2)}{d\log Q^2} = \quad & \frac{\alpha_{\rm em}}{2\pi}\int_x^1 \frac{dy}{y}\Big\{\sum_f e_f^2 P_{\gamma\leftarrow q}(y)\Big[q_f\Big(\frac{z}{y},Q^2\Big)+\bar q_f\Big(\frac{z}{y},Q^2\Big)\Big] \\ & + P_{\gamma\leftarrow\gamma}(y)\gamma\Big(\frac{z}{y},Q^2\Big)\Big\}\,. \end{aligned} \tag{19}$$

In the complete set of DGLAP equations this photon density is then again coupled to the quark and antiquark distributions:

$$\begin{aligned}\frac{dq_f(z,Q^2)}{d\log Q^2} = \quad & \frac{dq_f(z,Q^2)}{d\log Q^2}\Big|_{\rm QCD} + \frac{\alpha_{\rm em}}{2\pi}\int_x^1\frac{dy}{y}\delta P^{\rm QED}_{q\leftarrow q}(y) q_f\Big(\frac{z}{y},Q^2\Big) \\ + \quad & \frac{\alpha_{\rm em}}{2\pi}\int_x^1\frac{dy}{y}P_{q\leftarrow\gamma}(y)\gamma\Big(\frac{z}{y},Q^2\Big)\,. \end{aligned} \tag{20}$$

Due to the smallness of $\alpha_{\rm em}$ one would expect that the effect of photons on the quark and antiquark densities can be safely neglected, unless one is interested in high order perturbative corrections to the QCD splitting functions themselves.

Accordingly, we find two different approaches to DGLAP photons in the literature.

A first one, by Glück et al. [24] asserts, that we can neglect the photon density on the right hand side of the evolution equations. Then, at sufficiently large virtuality Q_0^2, the photon parton density can be calculated from the collinear splitting of quarks and antiquarks $q\to q\gamma, \bar q\to\bar q\gamma$.

$$\frac{d\gamma(z,Q^2)}{d\log Q^2} = \frac{\alpha_{\rm em}}{2\pi}\sum_f e_f^2\int_z^1\frac{dx}{x}P_{\gamma\leftarrow q}\Big(\frac{z}{x}\Big)\Big[q_f(x,Q^2)+\bar q_f(x,Q^2)\Big]\,. \tag{21}$$

This equation is easily integrated, and gives the photon parton density as

$$\begin{aligned}\gamma(z,Q^2) \;&=\; \sum_f\frac{\alpha_{\rm em}e_f^2}{2\pi}\int_{Q_0^2}^{Q^2}\frac{d\mu^2}{\mu^2}\int_z^1\frac{dx}{x}P_{\gamma\leftarrow q}\Big(\frac{z}{x}\Big)\Big[q_f(x,\mu^2)+\bar q_f(x,\mu^2)\Big]+\gamma(z,Q_0^2) \\ &=\; \frac{\alpha_{\rm em}}{2\pi}\int_{Q_0^2}^{Q^2}\frac{d\mu^2}{\mu^2}\int_z^1\frac{dx}{x}P_{\gamma\leftarrow q}\Big(\frac{z}{x}\Big)\frac{F_2(x,\mu^2)}{x}+\gamma(z,Q_0^2)\,. \end{aligned} \tag{22}$$

One is left to specify – from some model considerations – the photon density at some low scale $\gamma(z,Q_0^2)$, but one may hope that at very large $Q^2\gg Q_0^2\sim 1\,{\rm GeV}^2$ the part predicted perturbatively from quark and antiquark distributions dominates.

In addition to the above contribution from DGLAP splitting, Glück et al. also add the Weizsäcker-Williams flux from the coherent emission $p \to p\gamma^*$ without proton breakup as found in [23].

The Durham [25, 26] and NNPDF [16] groups have given a more involved treatment, in which the photon distribution is fully incorporated into the coupled DGLAP evolution equation. As usual with DGLAP evolution, the photon parton density at a starting scale $\gamma(z, Q_0^2)$ needs to be specified. While [25, 26] present model approaches, in Ref.[16] an ambitious attempt to obtain $\gamma(z, Q_0^2)$ from a fit to experimental data is found. Preliminary work by the CTEQ collaboration [27] is also based on QED corrected DGLAP equations, and attempts to fit the photon distribution from the prompt photon production $ep \to \gamma eX$ at HERA where in part of the phase space the Compton subprocess $e\gamma \to e\gamma$ contributes.

It should be noted, that in the approach of [25, 26], the input distribution $\gamma(z, Q_0^2)$ contains the coherent –or elastic– contribution with an intact proton in the final state. Notice that due to the proton form factors the integral over virtualities in the elastic case quickly converges, and the elastic contribution is basically independent of Q_0^2, as soon as $Q_0^2 \gtrsim 0.7\,\mathrm{GeV}^2$.

In the collinear approach the photon-photon contribution to inclusive cross section for dilepton production can be written as:

$$\frac{d\sigma^{(i,j)}}{dy_1 dy_2 d^2p_T} = \frac{1}{16\pi^2 (x_1 x_2 s)^2} \sum_{i,j} x_1\gamma^{(i)}(x_1, \mu^2) x_2\gamma^{(j)}(x_2, \mu^2) \overline{|\mathcal{M}_{\gamma\gamma\to l^+l^-}|^2}. \tag{23}$$

Here

$$\begin{aligned} x_1 &= \sqrt{\frac{p_T^2 + m_l^2}{s}} \Big(\exp(y_1) + \exp(y_2) \Big) \,, \\ x_2 &= \sqrt{\frac{p_T^2 + m_l^2}{s}} \Big(\exp(-y_1) + \exp(-y_2) \Big) \,. \end{aligned} \tag{24}$$

Above indices i and j denote $i, j = \mathrm{el}, \mathrm{in}$, i.e. they correspond to elastic or inelastic components similarly as for the k_T-factorization discussed in section below. The factorization scale is chosen as $\mu^2 = m_T^2 = p_T^2 + m_l^2$ (Renat?)

D. k_T-factorization approach

In this approach we start from the Feynman diagrams shown in Fig.**??**, and exploit the high-energy kinematics. Let the four-momenta of incoming protons be denoted p_A, p_B. At

high energies the proton masses can be neglected, so that $p_A^2 = p_B^2 = 0$, $2(p_A \cdot p_B) = s$.

The photon-fusion production mechanism in leptonic and hadronic reactions is in great detail reviewed in [23], where also many original references can be found. In the most general form, the invariant cross section is written as a convolution of density matrices of photons in the beam particles, and helicity amplitudes for the $\gamma^*\gamma^* \to l^+l^-$ process. In a high energy limit, where dileptons carry only a small fraction of the total center-of-mass energy, the density-matrix structure can be very much simplified, and there emerges a k_T-factorization representation of the cross section [28].

The unintegrated photon fluxes introduced in [28] can be expressed in terms of the hadronic tensor as

$$\mathcal{F}^{\rm in.el}_{\gamma^*\leftarrow A}(z,\boldsymbol{q}) = \frac{\alpha_{\rm em}}{\pi}\,(1-z)\left(\frac{\boldsymbol{q}^2}{\boldsymbol{q}^2 + z(M_X^2 - m_A^2) + z^2 m_A^2}\right)^2 \cdot \frac{p_B^\mu p_B^\nu}{s^2}\,W^{\rm in,el}_{\mu\nu}(M_X^2, Q^2) dM_X^2\,. \tag{25}$$

These unintegrated fluxes enter the cross section for dilepton production as

$$\frac{d\sigma^{(i,j)}}{dy_1 dy_2 d^2\boldsymbol{p}_1 d^2\boldsymbol{p}_2} = \int \frac{d^2\boldsymbol{q}_1}{\pi \boldsymbol{q}_1^2}\frac{d^2\boldsymbol{q}_2}{\pi \boldsymbol{q}_2^2}\mathcal{F}^{(i)}_{\gamma^*/A}(x_1,\boldsymbol{q}_1)\,\mathcal{F}^{(j)}_{\gamma^*/B}(x_2,\boldsymbol{q}_2)\frac{d\sigma^*(p_1,p_2;\boldsymbol{q}_1,\boldsymbol{q}_2)}{dy_1 dy_2 d^2\boldsymbol{p}_1 d^2\boldsymbol{p}_2}\,, \tag{26}$$

where the indices $i, j \in \{\rm el, in\}$ denote elastic or inelastic final states. The longitudinal momentum fractions of photons are obtained from the rapidities and transverse momenta of final state leptons as:

$$\begin{aligned} x_1 &= \sqrt{\frac{\boldsymbol{p}_1^2 + m_l^2}{s}}e^{y_1} + \sqrt{\frac{\boldsymbol{p}_2^2 + m_l^2}{s}}e^{y_2}\,, \\ x_2 &= \sqrt{\frac{\boldsymbol{p}_1^2 + m_l^2}{s}}e^{-y_1} + \sqrt{\frac{\boldsymbol{p}_2^2 + m_l^2}{s}}e^{-y_2}\,. \end{aligned} \tag{27}$$

The explicit form of the off-shell cross section $d\sigma^*(p_1,p_2;\boldsymbol{q}_1,\boldsymbol{q}_2)/dy_1 dy_2 d^2\boldsymbol{p}_1 d^2\boldsymbol{p}_2$ can be found in Refs. [4, 28].

E. Structure functions as input for unintegrated fluxes

The different parametrizations taken from the literature are labeled as:

- ALLM [29, 30]: This parametrization gives a very good fit to F_2 in most of the measured region.

- FJLLM [31]: This parametrization explicitly includes the nucleon resonances and gives an excellent fit of the CLAS data.

- SY [32]: This paramerization of Suri and Yennie from the early 1970's does not include QCD-DGLAP evolution. It is still today often used as one of the defaults in the LPAIR event generator.

- SU [33]: A parametrization which concentrates to give a good description at smallish and intermediate Q^2 at not too small x. A Vector-Meson-Dominance model inspired fit of F_2 at low Q^2, which is completed by the same NNLO MSTW structure function as above at large Q^2.

- LUX-like: a newly constructed parametrization, which at $Q^2 > 9\,\mathrm{GeV}^2$ uses an NNLO calculation of F_2 and F_L from NNLO MSTW 2008 partons [**?**]. It employs a useful code by the MSTW group [**?**] to calculate structure functions. At $Q^2 > 9\,\mathrm{GeV}^2$ this fit uses the parametrization of Bosted and Christy [34] in the resonance region, and a version of the ALLM fit published by the HERMES Collaboration [35] for the continuum region. It also uses information on the longitudinal structure function from SLAC [36]. As the fit is constructed closely following the LUXqed work Ref.[37].

III. EXAMPLE EXPERIMENTAL CONFIGURATION AND POSSIBLE BACKGROUND SOURCES

We assume collision setup from recent $p+\mathrm{Pb}$ run at the LHC, carried out at the centre-of-mass energy per nucleon pair $\sqrt{s_{NN}} = 8.16$ TeV. Since the energy per nucleon in the proton beam is larger than in the lead beam, the nucleon–nucleon centre-of-mass system has a rapidity in the laboratory frame of $+0.465$.

As an example of method's applicability, we will use the geometry of ATLAS [38] and CMS [39] detectors in the following. We also consider dimuon-channel only, however the integrated results for ee and $\mu\mu$ channels can be obtained by simply multiplying all cross-sections by a factor of two.

We start with applying minimum transverse momentum requirement of 4 GeV to both muons. This requirement is imposed to ensure high lepton reconstruction and triggering efficiency. Moreover, due to limited acceptance of the detectors, each muon is required to

Variable	Requirement
lepton transverse momentum, p_{T}^{ℓ}	> 4 GeV
lepton pseudorapidity, $\lvert\eta^{\ell}\rvert$	< 2.4
dilepton invariant mass, $m_{\ell^+\ell^-}$	> 10 GeV

TABLE I: Definition of the fiducial region used in the studies.

have a pseudorapidity (η^{ℓ}) that satisfies $|\eta^{\ell}| < 2.4$ condition. Our calculations are carried out for a minimum dilepton invariant mass $m_{\ell^+\ell^-} = 10$ GeV. Such a choice is due to removal of possible contamination from $\Upsilon(\to \ell^+\ell^-)$ photoproduction process. Summary of all selection requirements is presented in Table I

Possible background for this process can arise from inclusive lepton-pair production, e.g. from Drell–Yan process [40–43]. This processes would lead to disintegration of the incoming ion, and zero-degree calorimeters (ZDC) [44, 45] can be used to veto very-forward-going neutral fragments which would allow to fully reduce this background. Another background can arise from diffractive interactions, hence possibly mimicking signal topology. However, since the nucleus is a fragile object (with the nucleon binding energy of just 8 MeV) even the softest diffractive interaction will likely result in the emission of a few nucleons from the ion, detectable in the ZDC.

Another background category is the photon-induced process with resolved photon, i.e. $\gamma p \to Z/\gamma^* + X$ reaction. Here, the rapidity gap is expected to be smaller than in the signal process due to the additional particle production associated with the "photon remnant". Any other residual contamination of this process can be controlled using dedicated region, with a dilepton invariant mass around the Z-boson mass.

IV. RESULTS WITH COLLINEAR PHOTON-PDFS

We start with the calculation of the elastic contribution, $p + \mathrm{Pb} \to p + \mathrm{Pb} + \ell^+\ell^-$. In this case the photon flux becomes:

$$f_\gamma^p(x, \mu) = f_\gamma^p(x) \tag{28}$$

and the following parameterization is used []:

$$f_\gamma^p(x) = \frac{\alpha}{\pi}\left(\frac{1-x+0.5x^2}{x}\right)\left(\frac{A+3}{A-1}\log A - \frac{17}{6} - \frac{4}{3A} + \frac{1}{6A^2}\right) \ , \tag{29}$$

where $A = 1 + \frac{Q_0^2(1-x)}{xm_p^2}$ and $Q_0^2 = 0.71$ GeV^2.

The results for the elastic case are cross-checked with the calculation from STARlight MC and a good agreement is found: $\sigma_{fid}^{\rm el} = 17.5$ nb, whereas $\sigma_{fid}^{\rm STARlight} = 17.0$ nb. Both calculations are also corrected by a factor $S^2 = 0.96$ which takes into account the requirement that there be no hadronic interactions between the proton and the ion. This is calculated using STARlight, where the hard-sphere proton–nucleus requirement [46] is used.

Next, for the inelastic case ($\gamma p \to \ell^+\ell^- + X$), several recent parameterizations of the photon parton distributions are studied: CT14qed [15], LUXqed17 [37] and NNPDF3.1luxQED [47]. Comparison of several lepton kinematic distributions between different photon-PDFs are shown in Fig. 2,3,4,5.

The integrated fiducial cross-sections are summarized in Tab. II.

(some discussion here...)

Contribution	$p_T(\ell) > 4$ GeV	$p_T(\ell) > 4$ GeV, $\lvert\eta(\ell)\rvert < 2.4$, $M(\ell^+\ell^-) > 10$ GeV
$\gamma_{el}\gamma_{el}$ [$b_{min} = 0.7fm$]	45.5(2) nb	17.3(1) nb
$\gamma_{el}\gamma_{el}$ [Electric]	44.9(1) nb	17.5(1) nb
$\gamma_{el}\gamma_{el}$ [DZ]	53.3(1) nb	19.4(1) nb
$\gamma_{el}\gamma_{el}$ [CT14qed]	48.4(1) nb	17.6(1) nb
$\gamma_{inc}\gamma_{el}$ [CT14qed]	98.0(1) nb	39.7(1) nb
$\gamma_{inc}\gamma_{el}$ [LUXqed17]	105.8(1) nb	44.1(1) nb
$\gamma_{inc}\gamma_{el}$ [NNPDF3.1luxqed]	115.6(1) nb	45.9(1) nb
$\gamma_{inc}\gamma_{el}$ [HKR16qed]	121.6(1) nb	49.4(1) nb

TABLE II: Cross sections for different contributions

It should be made clear, that the calculations with collinear photons (at lowest order) produce leptons that are back-to-back in transverse kinematics. Therefore, to take the effect of inelastic photon virtuality into account, a dedicated parton shower algorithm should be used.

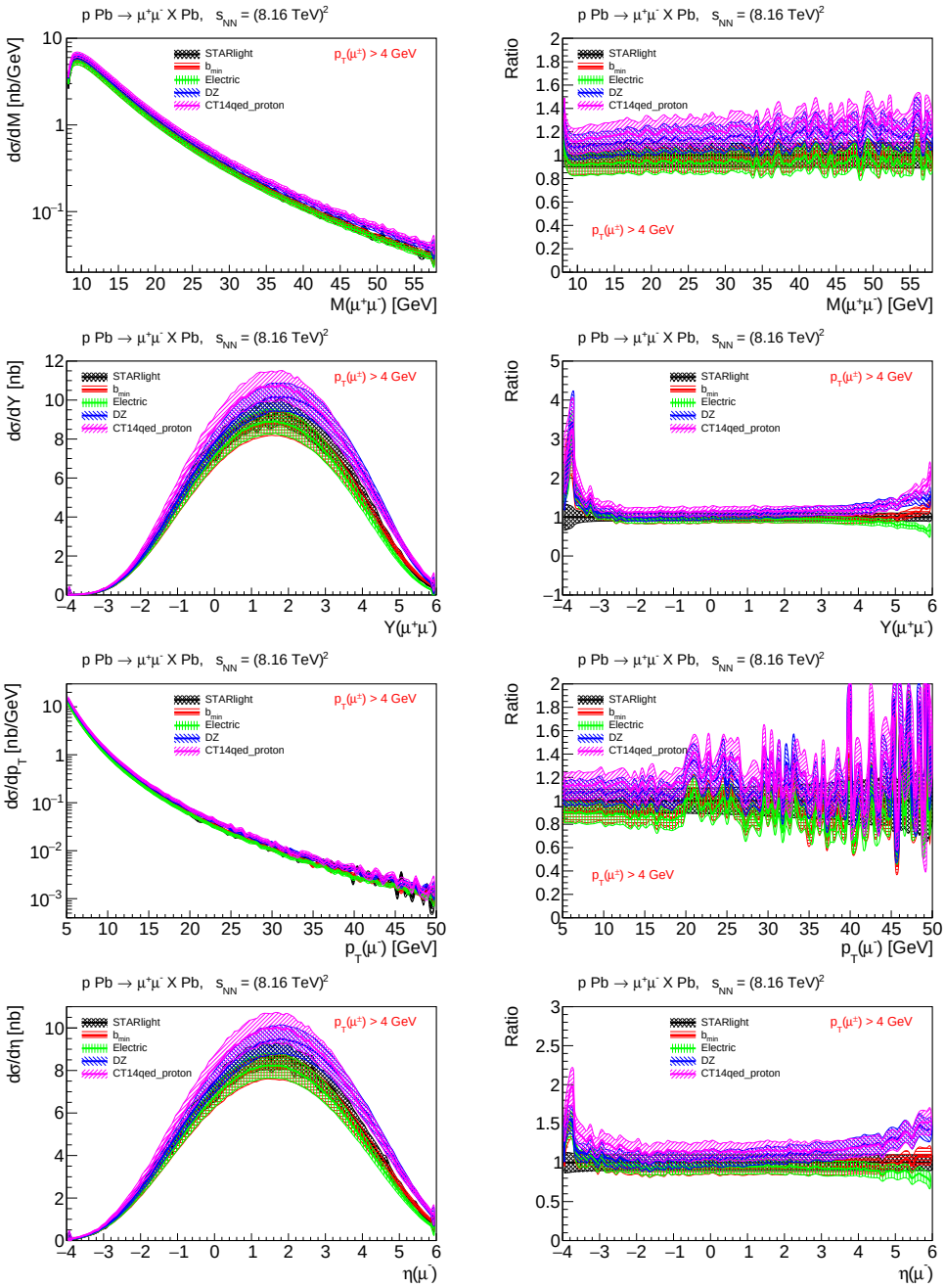

FIG. 2: Elastic distributions (the only cut is on leptons p_T)

(mention we don't want to do extra PS; we would rather stick to kt factorization)

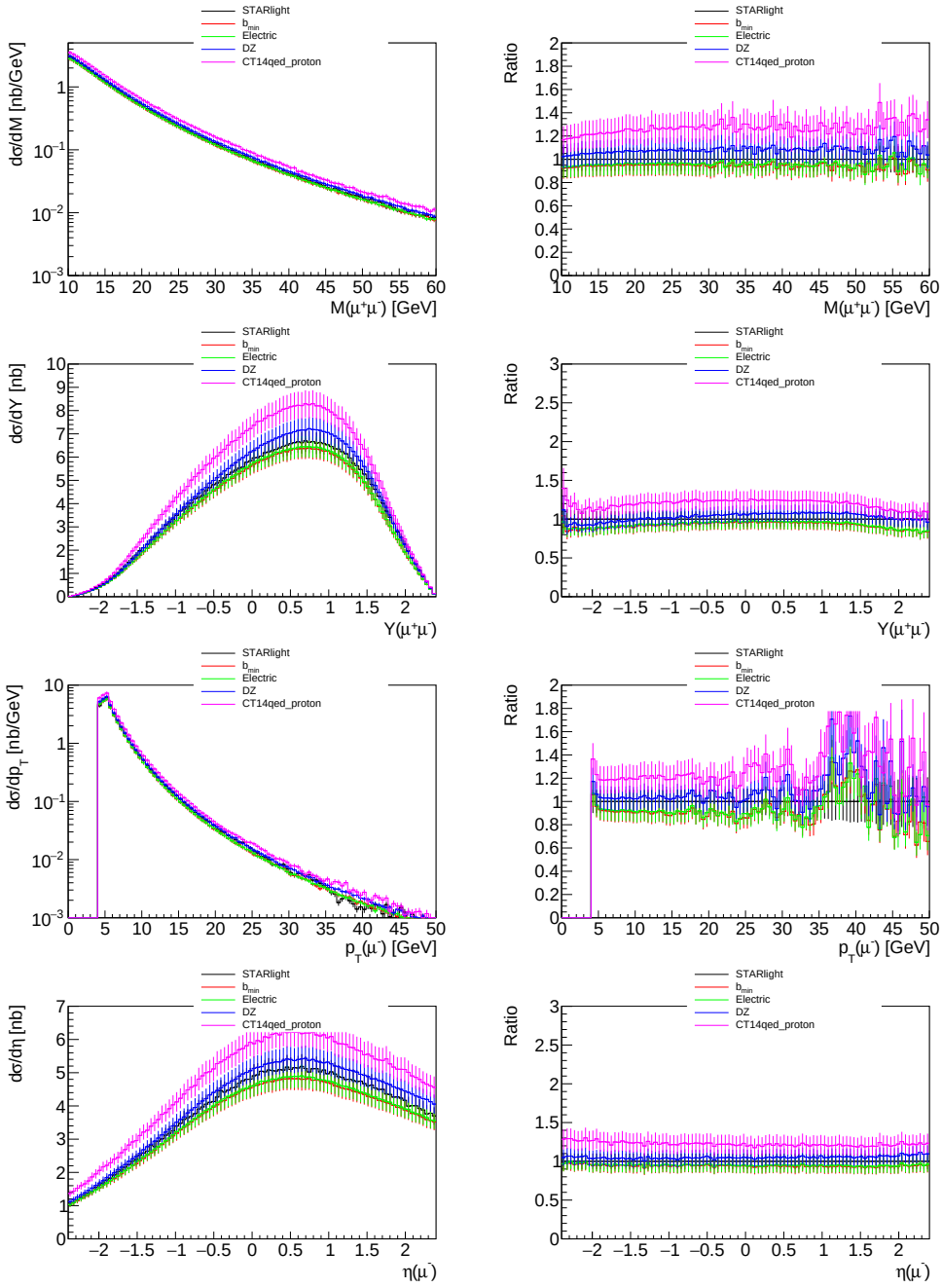

FIG. 3: Elastic distributions (fiducial region)

V. RESULTS INCLUDING PHOTON TRANSVERSE MOMENTUM

VI. DISCUSSION

We take the opportunity to calculate expected number of events for realistic assumption on total integrated luminosity. based on the previous pPb runs at the LHC, we assume

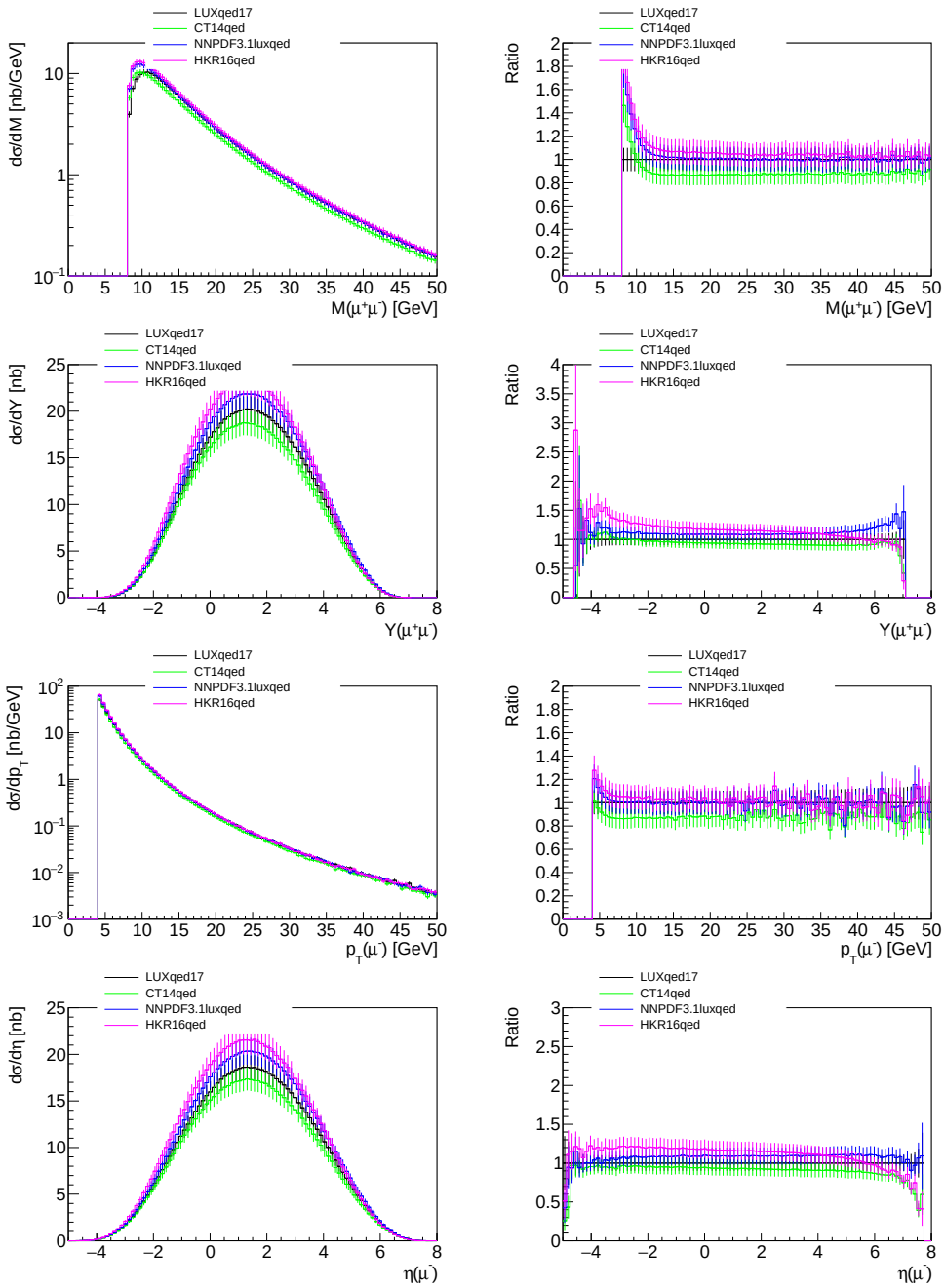

FIG. 4: Inclusive distributions (the only cut is on leptons p_T)

$\int Ldt = 200$ nb^{-1}.

(show some table(s) here)

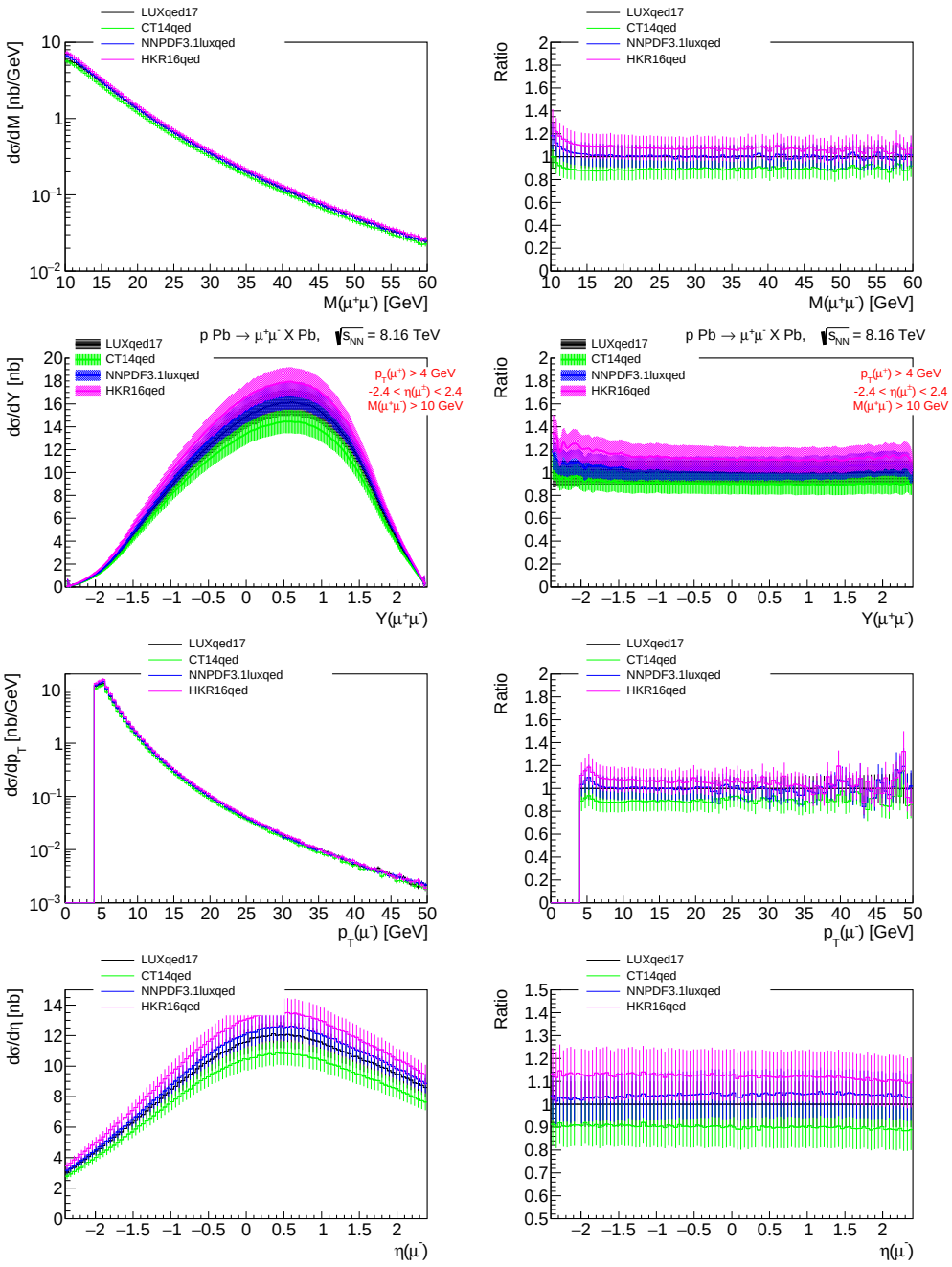

FIG. 5: Inclusive distributions (fiducial regoin)

VII. SUMMARY

In summary, we propose a method that would unambiguously allow to test and constrain the photon parton distribution at LHC energies.

contribution	$\sqrt{s_{NN}}$ = 8.16 TeV	$\sqrt{s_{NN}}$ = 8.16 TeV
	without cuts	$p_T > 4$ GeV, $\|y\| < 2.4$, $M_{l^+l^-} > 10$ GeV
LUX-like F2+FL $\gamma_{in}\gamma_{el}$	42.57	17.07
LUX-like F2 $\gamma_{in}\gamma_{el}$	43.58	17.44
ALLM97 F2 $\gamma_{in}\gamma_{el}$	41.72	16.43
Fiore et al. (parametrization of JLAB data) $\gamma_{in}\gamma_{el}$	45.24	18.36
SU F2 $\gamma_{in}\gamma_{el}$	41.72	16.70
SY F2 $\gamma_{in}\gamma_{el}$	40.38	15.99
Elastic- Elastic $\gamma_{el}\gamma_{el}$	47,89	18.26

TABLE III: Cross sections (in nb) for different contributions and different structure functions: LUX-like, ALLM97, Fiore, SU and SY. (the cross section was scaled by factors: 0.96 (elastic-elastic); 0.95 (elastic-inelastic) for proton-ion absorption (multiple interactions))

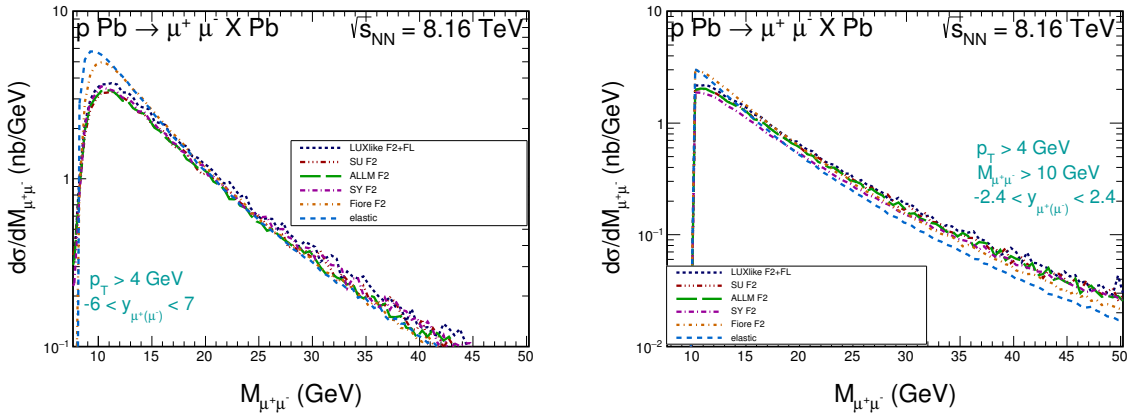

FIG. 6: The elastic - elastic and the inelastic-elastic contribution to dilepton invariant mass distributions for different structure functions. In the left panel we show the results for the whole phase space, while in the right panel only for the fiducial region.

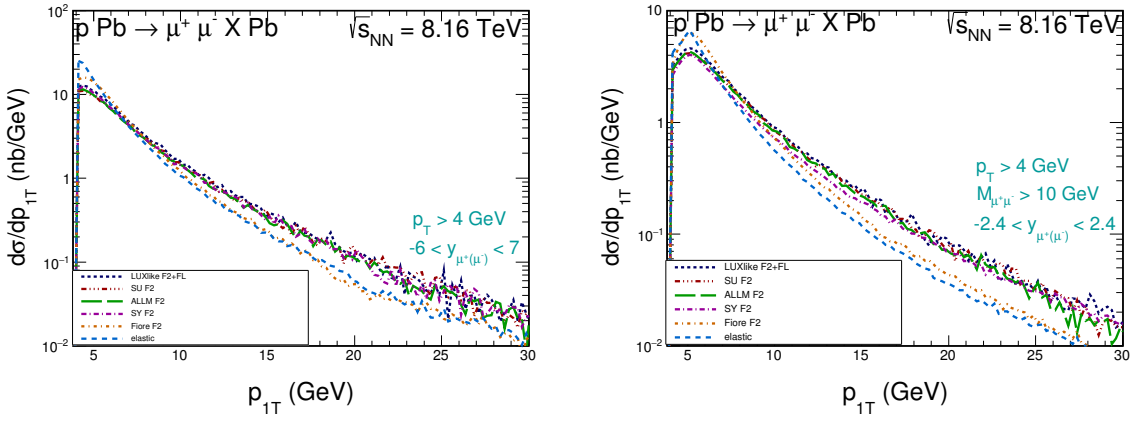

FIG. 7: Transverse momentum distribution of μ^+ or μ^- for elastic - elastic and inelastic - elastic different structure functions: LUX-like, ALLM97, Fiore at all., SU and SY (in the left panel we show the results for the whole phase space, while in the right panel only for the fiducial region).

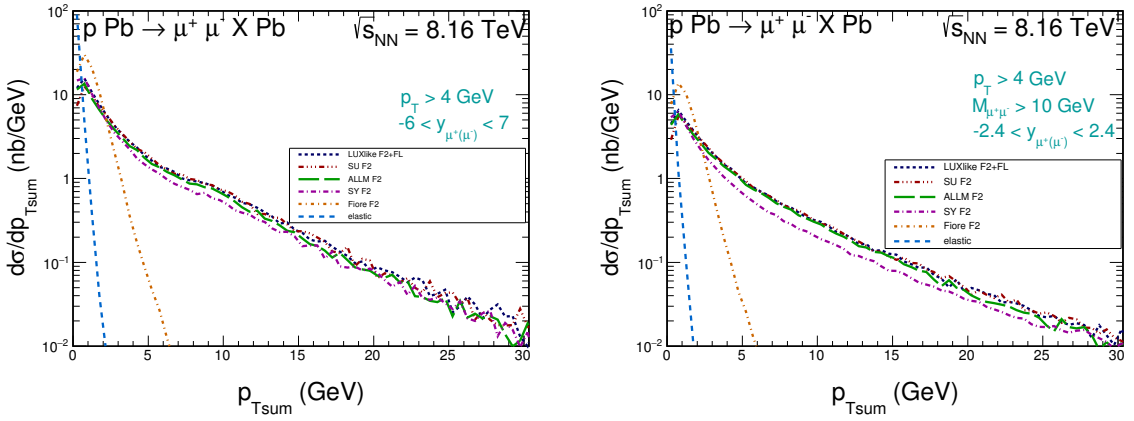

FIG. 8: Distribution in transverse momentum of the $\mu^+\mu^-$ pairs for elastic - elastic and inelastic-elastic contributions for different structure functions: LUX-like, ALLM97, Fiore at all., SU and SY. (in the left panel we show the results for the whole phase space, while in the right panel only for the fiducial region).

References

[1] ATLAS Collaboration, G. Aad et al., *Measurement of the low-mass Drell-Yan differential cross section at $\sqrt{s} = 7$ TeV using the ATLAS detector*, JHEP **06** (2014) 112, arXiv:1404.1212 [hep-ex].

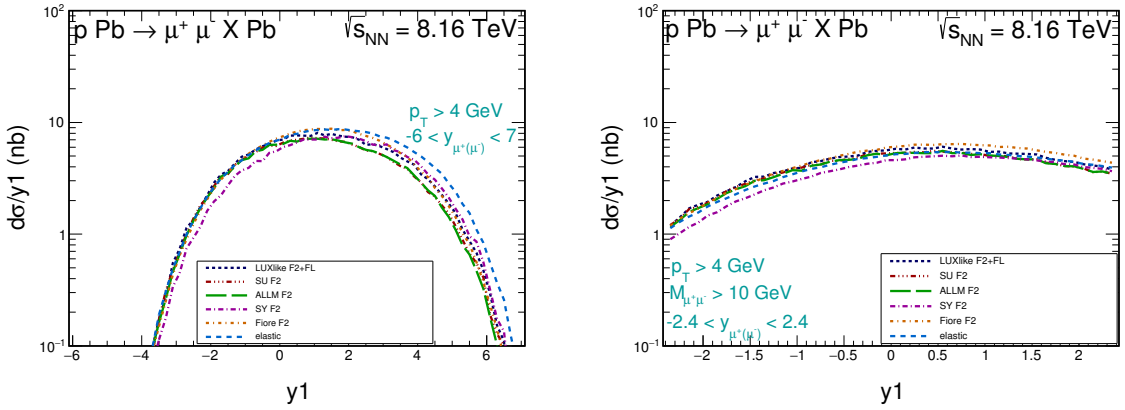

FIG. 9: Rapidity distribution of μ^+ or μ^- leptons for elastic - elastic and inelastic-elastic contributions for different structure functions: LUX-like, ALLM97, Fiore at all., SU and SY. (in the left panel we show the results for the whole phase space, while in the right panel only for the fiducial region).

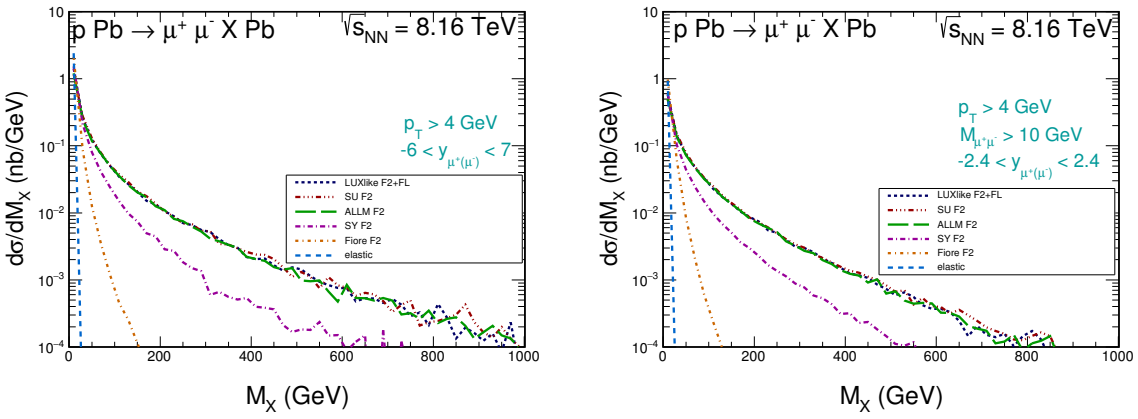

FIG. 10: Missing mass distributions for eleastic-elastic photon-photon contributions and elastic-inelastic photon-photon contributions for different structure functions: LUX-like, ALLM97, Fiore at all., SU and SY. (in the left panel we show the results for the whole phase space, while in the right panel only for the fiducial region).

[2] ATLAS Collaboration, G. Aad et al., *Measurement of the double-differential high-mass Drell-Yan cross section in pp collisions at $\sqrt{s} = 8$ TeV with the ATLAS detector*, JHEP **08** (2016) 009, `arXiv:1606.01736 [hep-ex]`.

[3] E. Accomando, J. Fiaschi, F. Hautmann, S. Moretti, and C. H. Shepherd-Themistocleous, *Photon-initiated production of a dilepton final state at the LHC: Cross section versus*

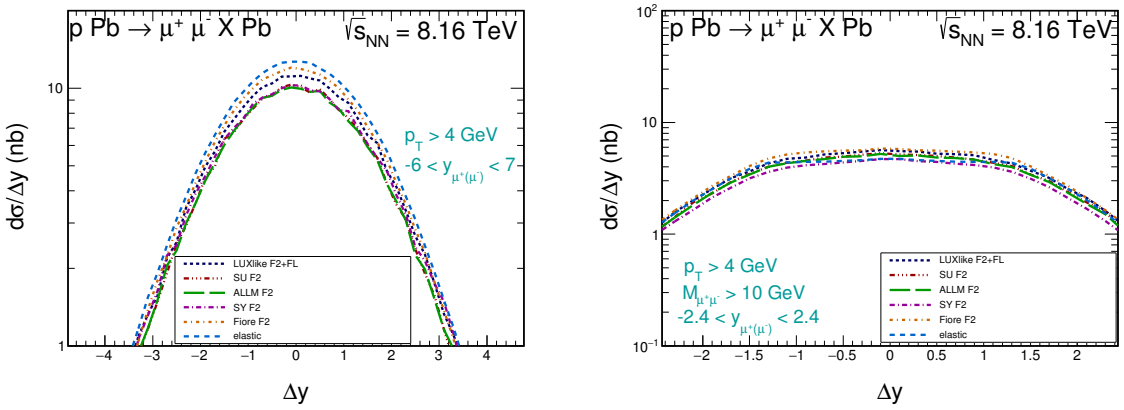

FIG. 11: Distribution in rapidity distance between $\mu^+\mu^-$ leptons. The calculation for the $\gamma - \gamma$ contribution was performed for different structure functions. The left panel shows results without cuts while the right panel shows results with ATLAS cuts.

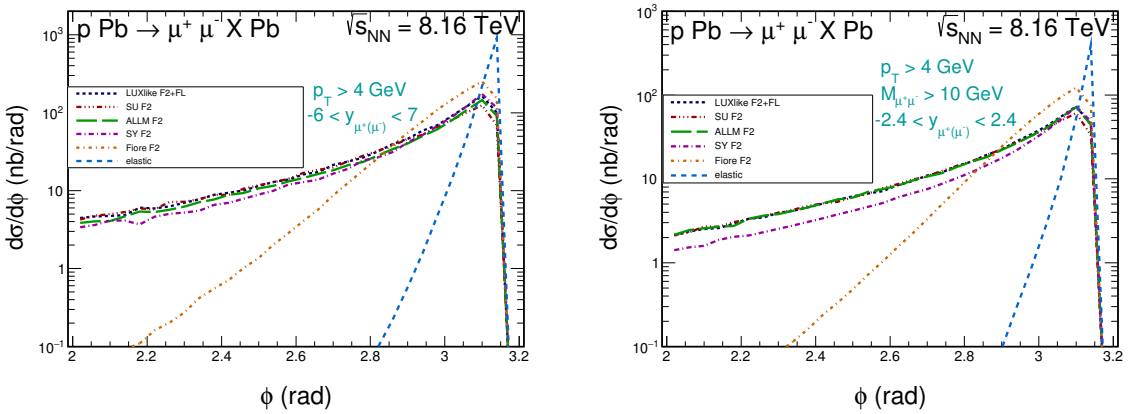

FIG. 12: Distributions for azimuthal angle between $\mu^+\mu^-$ leptons. (in the left panel we show the results for the whole phase space, while in the right panel only for the fiducial region).

forward-backward asymmetry studies, Phys. Rev. **D95** (2017) no. 3, 035014, arXiv:1606.06646 [hep-ph].

[4] M. Luszczak, W. Schafer, and A. Szczurek, *Two-photon dilepton production in proton-proton collisions: two alternative approaches*, Phys. Rev. **D93** (2016) no. 7, 074018, arXiv:1510.00294 [hep-ph].

[5] L. A. Harland-Lang, V. A. Khoze, and M. G. Ryskin, *The photon PDF in events with rapidity gaps*, Eur. Phys. J. **C76** (2016) no. 5, 255, arXiv:1601.03772 [hep-ph].

[6] M. Luszczak, A. Szczurek, and C. Royon, W^+W^- *pair production in proton-proton*

collisions: small missing terms, JHEP **02** (2015) 098, arXiv:1409.1803 [hep-ph].

[7] A. Denner, S. Dittmaier, M. Hecht, and C. Pasold, *NLO QCD and electroweak corrections to $Z + \gamma$ production with leptonic Z-boson decays*, JHEP **02** (2016) 057, arXiv:1510.08742 [hep-ph].

[8] M. Dyndal and L. Schoeffel, *Four-lepton production from photon-induced reactions in pp collisions at the LHC*, Acta Phys. Polon. **B47** (2016) 1645, arXiv:1511.02065 [hep-ph].

[9] M. Ababekri, S. Dulat, J. Isaacson, C. Schmidt, and C. P. Yuan, *Implication of CMS data on photon PDFs*, arXiv:1603.04874 [hep-ph].

[10] B. Biedermann, M. Billoni, A. Denner, S. Dittmaier, L. Hofer, B. Jger, and L. Salfelder, *Next-to-leading-order electroweak corrections to $pp \to W^+W^- \to 4$ leptons at the LHC*, JHEP **06** (2016) 065, arXiv:1605.03419 [hep-ph].

[11] B. Biedermann, A. Denner, S. Dittmaier, L. Hofer, and B. Jger, *Electroweak corrections to $pp \to \mu^+\mu^- e^+ e^- + X$ at the LHC: a Higgs background study*, Phys. Rev. Lett. **116** (2016) no. 16, 161803, arXiv:1601.07787 [hep-ph].

[12] Y. Wang, R.-Y. Zhang, W.-G. Ma, X.-Z. Li, and L. Guo, *QCD and electroweak corrections to ZZ+jet production with Z -boson leptonic decays at the LHC*, Phys. Rev. **D94** (2016) no. 1, 013011, arXiv:1604.04080 [hep-ph].

[13] M. Luszczak, W. Schafer, and A. Szczurek, *Production of W^+W^- pairs via $\gamma^*\gamma^* \to W^+W^-$ subprocess with photon transverse momenta*, JHEP **05** (2018) 064, arXiv:1802.03244 [hep-ph].

[14] A. Manohar, P. Nason, G. P. Salam, and G. Zanderighi, *How bright is the proton? A precise determination of the photon parton distribution function*, Phys. Rev. Lett. **117** (2016) no. 24, 242002, arXiv:1607.04266 [hep-ph].

[15] C. Schmidt, J. Pumplin, D. Stump, and C. P. Yuan, *CT14QED parton distribution functions from isolated photon production in deep inelastic scattering*, Phys. Rev. **D93** (2016) no. 11, 114015, arXiv:1509.02905 [hep-ph].

[16] NNPDF Collaboration, R. D. Ball, V. Bertone, S. Carrazza, L. Del Debbio, S. Forte, A. Guffanti, N. P. Hartland, and J. Rojo, *Parton distributions with QED corrections*, Nucl. Phys. **B877** (2013) 290–320, arXiv:1308.0598 [hep-ph].

[17] xFitter Developers' Team Collaboration, F. Giuli et al., *The photon PDF from high-mass Drell-Yan data at the LHC*, Eur. Phys. J. **C77** (2017) no. 6, 400, arXiv:1701.08553

[hep-ph].

[18] ATLAS Collaboration, G. Aad et al., *Measurement of exclusive $\gamma\gamma \to \ell^+\ell^-$ production in proton-proton collisions at $\sqrt{s} = 7$ TeV with the ATLAS detector*, Phys. Lett. **B749** (2015) 242–261, arXiv:1506.07098 [hep-ex].

[19] ATLAS Collaboration, M. Aaboud et al., *Measurement of the exclusive $\gamma\gamma \to \mu^+\mu^-$ process in proton-proton collisions at $\sqrt{s} = 13$ TeV with the ATLAS detector*, Phys. Lett. **B777** (2018) 303–323, arXiv:1708.04053 [hep-ex].

[20] CMS Collaboration, S. Chatrchyan et al., *Exclusive photon-photon production of muon pairs in proton-proton collisions at $\sqrt{s} = 7$ TeV*, JHEP **01** (2012) 052, arXiv:1111.5536 [hep-ex].

[21] CMS Collaboration, S. Chatrchyan et al., *Search for exclusive or semi-exclusive photon pair production and observation of exclusive and semi-exclusive electron pair production in pp collisions at $\sqrt{s} = 7$ TeV*, JHEP **11** (2012) 080, arXiv:1209.1666 [hep-ex].

[22] CMS, TOTEM Collaboration, A. M. Sirunyan et al., *Observation of proton-tagged, central (semi)exclusive production of high-mass lepton pairs in pp collisions at 13 TeV with the CMS-TOTEM precision proton spectrometer*, Submitted to: JHEP (2018) , arXiv:1803.04496 [hep-ex].

[23] V. M. Budnev, I. F. Ginzburg, G. V. Meledin, and V. G. Serbo, *The two photon particle production mechanism. Physical problems. Applications. Equivalent photon approximation*, Phys. Rept. **15** (1975) 181.

[24] M. Gluck, C. Pisano, and E. Reya, *The Polarized and unpolarized photon content of the nucleon*, Phys. Lett. **B540** (2002) 75–80, arXiv:hep-ph/0206126 [hep-ph].

[25] A. D. Martin, R. G. Roberts, W. J. Stirling, and R. S. Thorne, *Parton distributions incorporating QED contributions*, Eur. Phys. J. **C39** (2005) 155–161, arXiv:hep-ph/0411040 [hep-ph].

[26] A. D. Martin and M. G. Ryskin, *The photon PDF of the proton*, Eur. Phys. J. **C74** (2014) 3040, arXiv:1406.2118 [hep-ph].

[27] C. Schmidt, J. Pumplin, D. Stump, and C. P. Yuan, *QED effects and Photon PDF in the CTEQ-TEA Global Analysis*, PoS **DIS2014** (2014) 054.

[28] G. G. da Silveira, L. Forthomme, K. Piotrzkowski, W. Schfer, and A. Szczurek, *Central production via photon-photon fusion in proton-proton collisions with proton dissociation*,

JHEP **02** (2015) 159, arXiv:1409.1541 [hep-ph].

[29] H. Abramowicz, E. M. Levin, A. Levy, and U. Maor, *A Parametrization of sigma-T (gamma* p) above the resonance region Q**2 ¿= 0*, Phys. Lett. **B269** (1991) 465–476.

[30] H. Abramowicz and A. Levy, *The ALLM parameterization of sigma(tot)(gamma* p): An Update*, arXiv:hep-ph/9712415 [hep-ph].

[31] R. Fiore, A. Flachi, L. L. Jenkovszky, A. I. Lengyel, and V. K. Magas, *Explicit model realizing parton hadron duality*, Eur. Phys. J. **A15** (2002) 505–515, arXiv:hep-ph/0206027 [hep-ph].

[32] A. Suri and D. R. Yennie, *THE SPACE-TIME PHENOMENOLOGY OF PHOTON ABSORPTION AND INELASTIC ELECTRON SCATTERING*, Annals Phys. **72** (1972) 243.

[33] A. Szczurek and V. Uleshchenko, *Nonpartonic components in the nucleon structure functions at small Q**2 in the broad range of x*, Eur. Phys. J. **C12** (2000) 663–671, arXiv:hep-ph/9904288 [hep-ph].

[34] P. E. Bosted and M. E. Christy, *Empirical fit to inelastic electron-deuteron and electron-neutron resonance region transverse cross-sections*, Phys. Rev. **C77** (2008) 065206, arXiv:0711.0159 [hep-ph].

[35] HERMES Collaboration, A. Airapetian et al., *Inclusive Measurements of Inelastic Electron and Positron Scattering from Unpolarized Hydrogen and Deuterium Targets*, JHEP **05** (2011) 126, arXiv:1103.5704 [hep-ex].

[36] E143 Collaboration, K. Abe et al., *Measurements of R = σ(L) / σ(T) for 0.03 ¡ x ¡ 0.1 and fit to world data*, Phys. Lett. **B452** (1999) 194–200, arXiv:hep-ex/9808028 [hep-ex].

[37] A. V. Manohar, P. Nason, G. P. Salam, and G. Zanderighi, *The Photon Content of the Proton*, JHEP **12** (2017) 046, arXiv:1708.01256 [hep-ph].

[38] ATLAS Collaboration, G. Aad et al., *The ATLAS Experiment at the CERN Large Hadron Collider*, JINST **3** (2008) S08003.

[39] CMS Collaboration, S. Chatrchyan et al., *The CMS Experiment at the CERN LHC*, JINST **3** (2008) S08004.

[40] S. D. Drell and T.-M. Yan, *Massive Lepton Pair Production in Hadron-Hadron Collisions at High-Energies*, Phys. Rev. Lett. **25** (1970) 316–320. [Erratum: Phys. Rev. Lett.25,902(1970)].

[41] ATLAS Collaboration, G. Aad et al., *Z boson production in p+Pb collisions at* $\sqrt{s_{NN}} = 5.02$ *TeV measured with the ATLAS detector*, Phys. Rev. **C92** (2015) no. 4, 044915, arXiv:1507.06232 [hep-ex].

[42] CMS Collaboration, V. Khachatryan et al., *Study of Z boson production in pPb collisions at* $\sqrt{s_{NN}} = 5.02$ *TeV*, Phys. Lett. **B759** (2016) 36–57, arXiv:1512.06461 [hep-ex].

[43] ALICE Collaboration, J. Adam et al., *W and Z boson production in p-Pb collisions at* $\sqrt{s_{\rm NN}}$ *= 5.02 TeV*, JHEP **02** (2017) 077, arXiv:1611.03002 [nucl-ex].

[44] ALICE Collaboration, G. Dellacasa et al., *ALICE technical design report of the zero degree calorimeter (ZDC)*, . CERN-LHCC-99-05.

[45] ATLAS Collaboration, *Zero degree calorimeters for ATLAS*, . CERN-LHCC-2007-01.

[46] S. R. Klein, J. Nystrand, J. Seger, Y. Gorbunov, and J. Butterworth, *STARlight: A Monte Carlo simulation program for ultra-peripheral collisions of relativistic ions*, Comput. Phys. Commun. **212** (2017) 258–268, arXiv:1607.03838 [hep-ph].

[47] NNPDF Collaboration, V. Bertone, S. Carrazza, N. P. Hartland, and J. Rojo, *Illuminating the photon content of the proton within a global PDF analysis*, arXiv:1712.07053 [hep-ph].